

# Multi-dimensional Sensitivity Analysis by Monte Carlo Method

By

Kazuo SHIN, Masahiro TAKASUGI and Tomonori HYODO

(Received December 24, 1985)

## Abstract

A multi-dimensional sensitivity analysis method is proposed for evaluating the neutron flux perturbation due to the variance in the total, total scattering and differential scattering cross sections of the medium. The method is formulated based on the Monte Carlo method. The method uses the perturbation theory where the neutron random paths are not changed, and the variation in the neutron weight is estimated to describe the flux perturbation due to cross section errors.

The method is applied to analyze the neutron scattering experiment in the gun-source geometry. It is shown through the analysis that a variety of the flux perturbation is caused at each scattering direction by the cross section errors.

## I. Introduction

It is very important for shielding designers of nuclear reactors to continue their efforts to improve the accuracy of cross section data to minimize uncertainties in the neutron transport calculations. Rigorous sensitivity calculations are needed to make data adjustment using benchmark experiment data.

Previously, we carried out scattering experiments<sup>1),2)</sup> in a gun-source geometry. The results of these experiments are considered to be very sensitive, not only to the total cross section  $\Sigma_t$  and the total scattering cross section  $\Sigma_s$ , but also to the differential scattering cross section  $\frac{\partial \Sigma_s}{\partial \Omega}$ . Only the Monte Carlo method is suitable as a sensitivity analysis method for this kind of experimental data, because the Monte Carlo method can reproduce the geometrical effect precisely.

Rief<sup>3)</sup> applied the Monte Carlo method to the sensitivity analysis for the first time. He analyzed our experimental data<sup>2)</sup> at "YAYOI", based on the variance in the data of  $\Sigma_t$  and  $\Sigma_s$ . Since that time, the Monte Carlo method has been often applied by him for the analysis of shielding benchmark experiments<sup>4)</sup> performed in multi-dimensional configurations.

An analysis by Gerstle et al<sup>5)</sup> was a very rare example, in which the angular

---

\* Department of Nuclear Engineering

distributions of secondary neutrons were taken into account. They analyzed the shielding problem in a fusion reactor by considering the variance in the angular distribution of neutron inelastic scatterings.

The objective of this paper is to describe a method for evaluating the flux perturbations which are caused by the variance in not only the data of  $\Sigma$ , and  $\Sigma$ , but also in the angular distribution  $\frac{\partial \Sigma_s}{\partial \Omega}$ . The method is formulated based on the multi-group Monte Carlo method which allows one to take the multidimensional effect into account. The proposed method estimates the flux perturbation as a variation in neutron weight as it follows random walk paths of unperturbed neutrons. Covariance among cross section data can be easily considered in the method, if a covariance matrix is given.

To test the effectiveness of the method, the method is applied to analyze the results of our neutron scattering experiment<sup>1)</sup> which was done in the gun-source geometry.

## II. Method

The neutron transport is traced by the multigroup Monte Carlo method. Scattering angles are sampled from discrete angles by Coveyou's technique<sup>2)</sup>. Straker's method<sup>3)</sup> for discrete sampling, which is usually used in the multigroup Monte Carlo calculation, is not used here. The Coveyou method makes it easier to evaluate the flux perturbation due to the variance in the angular distribution of scattered neutrons.

The point detector estimation is adopted for the flux calculation at a detector point. The flux perturbation is calculated at each collision point where the estimator is used for the flux calculation, as Monte Carlo history is traced along its path.

The variance in total cross sections, total scattering cross sections and angular distributions of scattered neutrons is considered simultaneously to enable the treatment of the covariance among these data.

### (1) Variation in Uncollided Flux

The variation in uncollided flux  $\phi_g^u$  of  $g$ -th group is caused by the variance in the total cross section, and is expressed as  $\Delta\phi_g^u$ . Then,

$$\Delta\phi_g^u/\phi_g^u = e^{-\Delta\Sigma_g^t t_0}, \quad (1)$$

where  $\Delta\Sigma_g^t$  = the variance in the total cross section,

and  $t_0$  = neutron pass length in the medium from the source to the detector.

### (2) Variation of Collision Point

The neutron flight path  $s$  between successive collisions is determined as

$$s = -\log r / \Sigma_g, \quad (2)$$

where  $r$  = a random number.

When the cross section  $\Sigma_g^f$  is varied, the value  $s$  becomes  $s + \Delta s$ . The variation  $\Delta s$  is written as

$$\Delta s/s = -\Delta \Sigma_g^f / \Sigma_g^f. \quad (3)$$

This variation of the collision point is considered in estimating the flux by the point estimator at the latest collision point. (See Eq. (5).) The effects on the flux by variation of the neutron flight path prior to the latest collision are taken into account only by varying the neutron weight factor. (See Eq. (7).)

### (3) Variation in Point Estimator

The contribution to the detector flux from the  $j$ -th collision point is written by the point estimator as

$$\phi_g^j = W_j \Sigma_{g'}^g(\mu) e^{-\Sigma_{g'}^g t_j / (\Sigma_{g'}^g l_j^2)}, \quad (4)$$

where  $t_j$  = neutron flight path in the medium along the direction from the  $j$ -th point to the detector,

$l_j$  = distance from the  $j$ -th point to the detector,

$\Sigma_{g'}^g(\mu)$  = differential scattering cross section at scattering angle  $\mu$  and from  $g$ -th group to  $g'$ -th group at  $j$ -th collision point,

and  $W_j$  = neutron weight factor.

The variation in  $\phi_g^j$  is introduced as

$$\phi_g^j + \Delta \phi_g^j = \frac{(W_j + \Delta W_j) (\Sigma_{g'}^g(\mu) + \Delta \Sigma_{g'}^g(\mu)) e^{-(\Sigma_{g'}^g + \Delta \Sigma_{g'}^g)(t_j + \Delta t_j)}}{(\Sigma_{g'}^g + \Delta \Sigma_{g'}^g) \cdot (l_j + \Delta l_j)^2}, \quad (5)$$

where the variance  $\Delta \Sigma_{g'}^g(\mu)$  includes both the variance in the total scattering cross section and in the angular distribution of the scattering. The variation  $\Delta l_j$  and  $\Delta t_j$  is introduced by the variation of the latest collision point described by Eq. (3).

The differential cross section  $\Sigma_{g'}^g(\mu)$  is assumed to be expanded by the Legendre polynomials as

$$\Sigma_{g'}^g(\mu) = \sum_{i=0}^n \frac{1}{4\pi} f_{g'}^g P_i(\mu), \quad (6)$$

where  $f_{g'}^g$  = total scattering cross section  $\Sigma_{g'}^g$ .

The variation in the weight  $W_j$  is caused by the accumulated effects of the variation in the neutron path,  $\Sigma_{g'}^g$ ,  $f_{g'}^g$  ( $l \neq 0$ ) and  $\Sigma_{g'}^g$  in the previous collisions, and is written explicitly as

$$(W_j + \Delta W_j) / W_j = \prod_{i=1}^{j-1} \left( \frac{\tilde{\omega}_i + \Delta \tilde{\omega}_i}{\tilde{\omega}_i} \right) \left( \frac{\tilde{W}_i + \Delta \tilde{W}_i}{\tilde{W}_i} \right) e^{-\Sigma_{g'}^g \Delta s_i}, \quad (7)$$

where  $(\tilde{\omega}_i + \Delta \tilde{\omega}_i) / \tilde{\omega}_i$  = variation caused by the variance  $\Delta f_{g'}^g$  (See Eq. (14).),

$(\tilde{W}_i + \Delta\tilde{W}_i)/\tilde{W}_i$  = variation caused by the variance  $\Delta\Sigma_{ii}^{g \rightarrow g'}$  and  $\Delta\Sigma_{ii}^g$  (See Eq. (10).),

and  $e^{-(\Sigma_{ii}^{g \rightarrow g'} \Delta s_i)}$  = variation caused by the variation  $\Delta s_i$  in Eq. (3) at the previous collision points.

If the variance is not large, Eq. (5) can be written as

$$\begin{aligned} \Delta\phi_{g'}^j / \phi_{g'}^j \simeq & \frac{\Delta W_j}{W_j} + \frac{\Delta\Sigma_{ii}^{g \rightarrow g'}(\mu)}{\Sigma_{ii}^{g \rightarrow g'}(\mu)} - \frac{\Delta\Sigma_{ij}^{g'}}{\Sigma_{ij}^{g'}} - 2 \frac{\Delta l_j}{l_j} \\ & - \Sigma_{ij}^{g'} t_j \left( \frac{\Delta\Sigma_{ij}^{g'}}{\Sigma_{ij}^{g'}} + \frac{\Delta t_j}{t_j} \right). \end{aligned} \quad (8)$$

#### (4) Variation in Emission Probability in Scattering

The probability that the neutron is scattered at the  $i$ -th point from  $g$ -th group to  $g'$ -th group is written as

$$P_i^{g \rightarrow g'} = \frac{\Sigma_{ii}^{g \rightarrow g'}}{\Sigma_{ii}^g}. \quad (9)$$

When variance is derived into  $\Sigma_{ii}^g$  and  $\Sigma_{ii}^{g \rightarrow g'}$ , neutron emission probability  $P_i^{g \rightarrow g'}$  is varied. This effect is evaluated at each collision point as the weight reduction by the following factor:

$$(\tilde{W}_i + \Delta\tilde{W}_i)/\tilde{W}_i = 1 + \Delta\Sigma_{ii}^{g \rightarrow g'} / \Sigma_{ii}^{g \rightarrow g'} - \Delta\Sigma_{ii}^g / \Sigma_{ii}^g. \quad (10)$$

#### (5) Variation in Weight Factor due to Change in Angular Distribution

The Probability that the neutron is scattered at the scattering angle  $\mu_k$ , which is one of the discrete angles, is written as follows by Coveyou's technique;

$$\tilde{\omega}_k = \frac{\sum_{l=0}^n f_l^{g \rightarrow g'} P_l(\mu_k)}{\sum_{l=0}^n (2l+1) \{P_l(\mu_k)\}^2}, \quad (11)$$

where  $\sum_{k=1}^n \tilde{\omega}_k = 1$ . (12)

When  $f_l^{g \rightarrow g'}$  is changed to  $f_l^{g \rightarrow g'} + \Delta f_l^{g \rightarrow g'}$ , then  $\tilde{\omega}_k$  becomes  $\tilde{\omega}_k + \Delta\tilde{\omega}_k$ . From Eq. (11),  $\Delta\tilde{\omega}_k$  can be written as

$$\Delta\tilde{\omega}_k = \frac{\sum_{l=0}^n \Delta f_l^{g \rightarrow g'} P_l(\mu_k)}{\sum_{l=0}^n (2l+1) \{P_l(\mu_k)\}^2}; \quad (13)$$

and the neutron weight variation at the collision point is written as

$$(\tilde{\omega}_i + \Delta\tilde{\omega}_i)/\tilde{\omega}_i = 1 + \frac{\sum_{l=0}^n \Delta f_l^{g \rightarrow g'} P_l(\mu_k)}{\sum_{l=0}^n f_l^{g \rightarrow g'} P_l(\mu_k)}. \quad (14)$$

### III. Examples of Test Calculation

The method described in the above chapter is applied in order to test the effectiveness of the method to the analysis of a neutron scattering experiment<sup>1)</sup> which was done with collimated neutrons from a  $^{252}\text{Cf}$  source. The experiment with a heavy concrete slab was chosen for this purpose from a variety of experiments already completed with several materials mentioned in References 1) and 2).

Fast neutron spectra transmitted through the 20-cm thick heavy concrete slab were given at directions of 0 deg., 60 deg. and 120 deg. with respect to the incident neutron direction. Figure 1 shows the experimental arrangement.

Group constants with  $P_8$  approximation were generated by the RADHEAT-V3

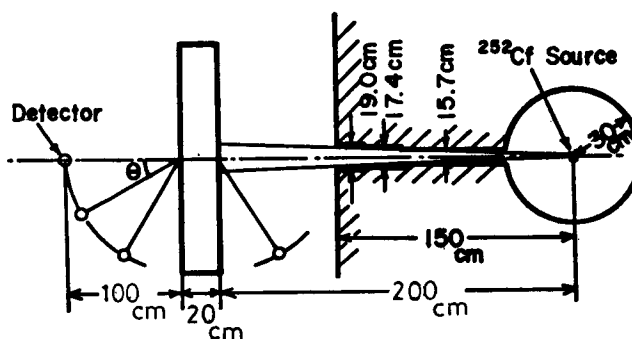


Fig. 1. Experimental arrangement.

Table I Energy Group Structure

Gcoup	Boundary (MeV)	Group	Boundary (MeV)
1	15	14	5.5
2	13	15	5.0
3	12	16	4.5
4	11	17	4.0
5	10	18	3.5
6	9.5	19	3.0
7	9.0	20	2.5
8	8.5	21	2.0
9	8.0	22	1.5
10	7.5	23	1.4
11	7.0	24	1.3
12	6.5	25	1.2
13	6.0	26	1.1
			1.0

Table II Atomic Compositions of Heavy Concrete\*

Elements	Weight %
S	47.5
Fe	41.4
Si	1.5
O	0.5
Ca	1.66
Al	0.15

\*Density is 4.0 g/cm<sup>3</sup>.

code system<sup>8)</sup> from pointwise cross section data in the ENDF/B-IV file<sup>9)</sup>. The group structure of the constants is shown in Table I. The atomic densities of elements in the heavy concrete are shown in Table II. Evaluated cross section data were not available for sulphur, so silicon data were used for sulphur data.

Figure 2 compares the spectra between the experiment and the multigroup Monte Carlo calculation. From the figure, the following can be pointed out: (1) At energies 1-2 MeV, a large discrepancy between the experiment and the calculation is seen in 0 deg. spectrum, but the discrepancy is small at the other directions. (2) In the energy range 3-5 MeV, the calculated spectrum is larger than the measured one at all directions. (3) In the energy range 5-7 MeV, a difference in structural shape is seen in the 0 deg. spectrum between the calculation and the experiment. The experimental spectrum is larger than the calculated one in the 60 deg. spectrum, but the reverse is the case at 120 deg. (4) At energies higher than 7 MeV, a discrepancy is

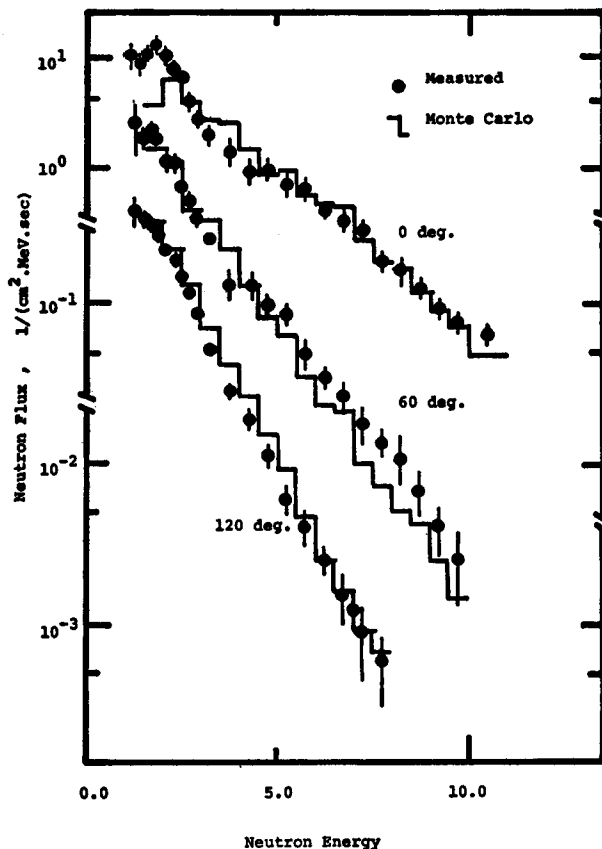


Fig. 2. Comparison of calculated and measured neutron spectra at 0, 60, and 120 deg. for the 20-cm heavy concrete slab.

seen between the experiment and the calculation only in the 60 deg. spectrum, where the measured values are larger than the calculated ones.

These discrepancies between the experiment and the calculation were considered<sup>1)</sup> due to errors in the cross section data of the calculation because silicon data were used in place of sulphur data. The quantitative analysis was performed to test the point.

According to BNL-325<sup>10)</sup>, the total cross section of sulphur in the energy range 3-5 MeV is about 1.2 times larger than that of silicon. Hence, the replacement of the sulphur data by the silicon data caused about a 20% underestimation of the sulphur cross section, which in turn caused about an 8% underestimation of the heavy concrete cross section. We checked the effect on the flux due to the increase in the total cross section which compensated for the underestimation. The results are shown in Table III for groups 16, 17 and 18 as the relative change in the fluxes of these groups. (See Table I.) The results in the table suggest that the Monte Carlo spectra will come closer to the measured ones if the cross sections are corrected.

Table III Sensitivity of Group Flux to Total Cross Section\*

	Percent Change in Flux (%)		
	0 Deg.	60 Deg.	120 Deg.
$\Delta\phi_{16}/\phi_{16}$	-27.6	-24.2	-12.0
$\Delta\phi_{17}/\phi_{17}$	-27.2	-28.5	-17.9
$\Delta\phi_{18}/\phi_{18}$	-29.0	-31.1	-20.4

\*) The 8% change in the total cross sections in the 16th, 17th and 18th groups.

Consider the discrepancies in the range 5-7 MeV. The difference in the spectral shape of the 0 deg. spectrum just corresponds to the difference in the structure of the total cross section between silicon and sulphur. This can be confirmed by comparing the silicon data in the ENDF/B-IV file with the sulphur data in BNL-325. Therefore, the calculation was not done for this problem.

The discrepancies between the calculation and the experiment observed in the 60 deg. and 120 deg. spectra at the energies 5-7 MeV seemed to be caused by an inaccuracy in the angular distribution of the scattering cross sections. The angular distribution at 4, 8 MeV is cited from BNL-400<sup>11)</sup> in Fig. 3 for the silicon and sulphur. From the figure it can be seen that the sulphur data is larger than the silicon data at 60 deg. in the laboratory system, but at 120 deg. the reverse is true. This kind of discrepancy in the pointwise data appears in group constants as errors in the coefficients

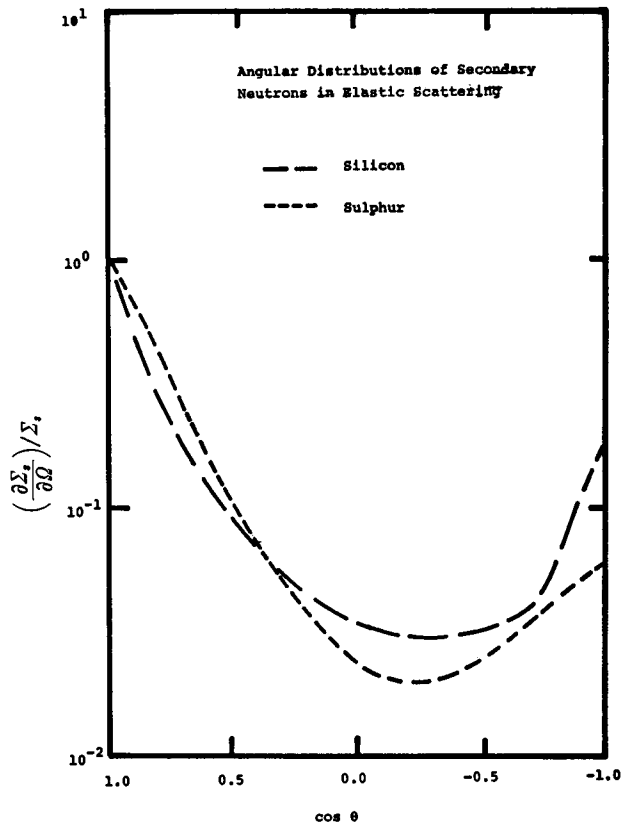


Fig. 3. Differential scattering cross section of silicon and sulphur at 4.8 MeV.

Table IV Sensitivity of Group Flux to Coefficient  $f_l$

$\Delta f_l = \alpha f_l$		Percent Change in the 14th Group Flux (%)		
$l$	$\alpha$ (%)	0 Deg.	60 Deg.	120 Deg.
1	10	1.0	10.6	-30.9
2	10	1.2	6.0	-6.7
3	-10	0.5	-2.7	-14.1
4	10	-0.3	3.0	0.4

of the  $P_l$  expansion.

The calculated flux perturbation, which corresponds to a 10% change in the coefficients  $f_l$  ( $l \neq 0$ ), is shown in Table IV. When the value of  $f_1$  or  $f_2$  is increased, the 60 deg. flux increases, but the 120 deg. flux decreases. The 0 deg. flux scarcely changes. Hence, the discrepancies in the 5-7 MeV region are attributed to errors



mainly in the coefficients  $f_1$  and  $f_2$ .

In the higher energy region, a similar analysis can be done. However, data for the differential scattering cross section of sulphur were not available for us at these energies, so the analysis was not carried out.

By calculations for other materials, the following tendency was observed. When the data of  $\Sigma_t$  and  $\Sigma_s$  were increased by the same amount, the 0 deg. flux decreased, but the fluxes at other directions were scarcely changed. Taking this fact into account, the discrepancy between the calculation and the experiment seen in the 0 deg. spectrum at 1-2 MeV (See Fig. 2.) may be explained by the overestimation of  $\Sigma_t$  and  $\Sigma_s$  by about the same amount as the replacement of the sulphur data was done by the silicon data.

#### IV Conclusion

A sensitivity analysis method for multi-dimensional geometries was formulated based on the Monte Carlo method and applied to the three dimensional experiment made in the gun-source geometry.

The following suggestions were obtained through the test calculation by the derived method.

- (1) The formulations given in this paper are useful for a multi-dimensional sensitivity analysis.
- (2) The variance in  $\Sigma_t$ ,  $\Sigma_s$ , and  $f_i$  caused a variety of the flux perturbation at each direction of 0 deg., 60 deg. and 120 deg.
- (3) The experimental data in the gun-source geometry is adequate for a systematic testing of various kinds of cross section data.

#### References

- 1) K. Shin et al., Mem. of Faculty of Engng., Kyoto Univ., Vol. XLIII, 331 (1981).
- 2) K. Shin et al., J. of Nucl. Sci. & Technol., 17, 37 (1980).
- 3) H. Rief, "An Attempt of Sensitivity Calculations in 3-D Geometries by Monte Carlo Techniques," Proceedings of the Specialists' Meeting on Sensitivity Studies and Shielding Benchmarks, pp. 68 OECD, Paris (1975).
- 4) H. Rief, "Three-Dimensional Effects in Sensitivity Studies", Proceedings of the Fifth International Conference on Reactor Shielding, pp. 112, Knoxville USA (1977).
- 5) S. A. Gerstl, "Sensitivity Profiles for Secondary Energy and Angular Distributions", Proceedings of the Fifth International Conference on Reactor Shielding, pp. 101, Knoxville USA (1977).
- 6) D. C. Irving et al., "O5R, A General-Purpose Monte Carlo Neutron Transport Code," USAEC Report ORNL-3622, Oak Ridge National Laboratory (1965).
- 7) E. A. Straker et al., "The MORSE Code-a Multigroup Neutron and Gamma-Ray Monte Carlo Transport Code," ORNL-4585, Oak Ridge National Laboratory (1970).
- 8) K. Koyama et al., "DADHEAT-V3; A Code System for General Coupled Neutron and Gamma-Ray Group Constants and Analyzing Radiation Transport," JAERI-M-7155, Japan

- Atomic Energy Research Institute (1977).
- 9) "ENDF/B Summary Documentation", BNL-NCS-17541 (ENDF-201), 2nd. ed. (ENDF/B-IV), D. Garber, Ed., available from the National Nuclear Data Center, Brookhaven National Laboratory (1975).
  - 10) R. R. Kinsey and V. McLane, "Neutron Cross Sections Vol. II; Neutron Cross Section Curves," Academic Press, New York (1981).
  - 11) D. I. Garber et al., "Angular Distributions in Neutron-Induced Reactions", BNL 400 Third Ed., National Cross Section Center, Brookhaven National Laboratory (1970).